# The distribution of methylated sulfur compounds, DMS and DMSP, in Canadian Subarctic and Arctic marine waters during summer, 2015

Tereza Jarníková [(1)], John Dacey[(2)], Martine Lizotte[(3)], Maurice Levasseur [(3)] and Philippe Tortell[(1,4,5)]

(1) Department of Earth, Ocean and Atmospheric Sciences, University of British Columbia, 2022 Main Mall, Vancouver BC, Canada V6T 1Z3

(2) Woods Hole Oceanographic Institution, Woods Hole, MA 02543.

(3) Université Laval, Department of Biology (Québec-Océan), Québec City, Québec, Canada.

(4) Department of Botany, University of British Columbia, 6270 University Blvd., Vancouver BC, Canada V6T 1Z4

(5) Peter Wall Institute for Advanced Studies, University of British Columbia, 6330 Crescent Blvd., Vancouver BC, Canada V6T 1Z4

**Correspondence to: Tereza Jarníková (tjarniko@eoas.ubc.ca)**

**Abstract**

**We present seawater concentrations of dimethylsulfide (DMS), and dimethylsulfoniopropionate (DMSP) measured across a transect from the Labrador Sea to the Canadian Arctic Archipelago, during summer 2015. Using an automated ship-board gas chromatography system, and a membrane-inlet mass spectrometer, we measured a wide range of DMS (~1 nM to 18nM) and DMSP (~1 nM to 150 nM) concentrations. The highest DMS and DMSP concentrations occurred in a localized region of Baffin Bay, where surface waters were characterized by high chlorophyll *a* (chl *a*) fluorescence, indicative of elevated phytoplankton biomass. Across the full sampling transect, there were only weak relationships between DMS/P, chl *a* fluorescence and other measured variables, including positive relationships between DMSP:chl *a* ratios and several taxonomic marker pigments, and elevated DMS/P concentrations in partially ice-covered areas. Our high spatial resolution measurements allowed us to examine DMS variability over small scales (<1 km), documenting strong DMS concentration gradients across surface hydrographic frontal features. Our new observations fill in an important observational gap in the Arctic Ocean, and provide additional information on sea-air DMS fluxes from this ocean region. In addition, this study constitutes a significant contribution to the existing Arctic DMS/P dataset, and provide a baseline for future measurements in the region.**

## 1. Introduction

The trace gas dimethylsulfide (DMS), a degradation product of the algal metabolite dimethylsulfoniopropionate (DMSP), is the largest natural source of sulfur to the atmosphere, accounting for over 90% of global biogenic sulfur emissions (Simó, 2001). Atmospheric DMS is rapidly oxidized to sulfate aerosols that act as cloud condensation nuclei (CCN), backscattering incoming radiation, increasing the albedo of low-altitude clouds and potentially cooling the Earth (Charlson et al., 1987). The seminal CLAW hypothesis proposed by Charlson et al. (1987) suggests that this negative radiative forcing will have cascading effects on marine primary productivity, leading to a DMS-mediated climate feedback loop. Although more recent work has disputed the mechanism of this biologically-mediated climate feedback (Quinn and Bates, 2011), the CLAW hypothesis has provided motivation for the widespread measurement of DMS in the global ocean over the past thirty years.

Beyond their potential role in regional climate forcing, DMS and DMSP also play critical ecological roles in marine microbial metabolism and food-web dynamics (for a complete overview; see Stefels et al., 2007). DMSP is believed to serve numerous physiological functions in phytoplankton, with suggested roles as an osmolyte, an anti-oxidant, and a cryoprotectant under different environmental conditions. Sunda et al. (2002) suggested that oxidative stressors, such as high solar radiation or iron limitation, may stimulate DMSP production in certain phytoplankton species. The production of this molecule is largely species-dependent, and can vary by three orders of magnitude among phytoplankton groups, with the highest intracellular concentrations typically reported in

dinoflagellates and haptophytes, and lower concentrations in diatoms (Keller, 1989).

After synthesis, DMSP can be cleaved to DMS and acrylate within algal cells, or by heterotrophic bacteria acting on the dissolved DMSP ($DMSP_d$) pool in the water column (Zubkov et al., 2001). The release of DMSP into the water column is believed to be enhanced in physiologically stressed or senescent phytoplankton (Malin et al., 1998), and can be stimulated by zooplankton grazing and viral lysis (Evans et al., 2007). Bacteria can also utilize $DMSP_d$ as a sulfur source for protein synthesis (Kiene et al., 2000), but this pathway does not lead to DMS release. The DMS yield of bacterial DMSP metabolism (i.e. the fraction of consumed DMSP that is converted to DMS) varies significantly, and may be influenced by the relative supply and demand of reduced sulfur and carbon for bacterial growth (Kiene and Linn, 2000).

In environments with low anthropogenic aerosol concentrations, understanding the impact of natural aerosol sources on cloud formation is critical to correctly estimating climate forcing (Carslaw et al., 2013). Modeling studies have suggested that DMS emissions could exert a particularly significant influence on CCN formation and regional climate in polar regions, due to the low background concentrations of atmospheric aerosols at high latitudes (Woodhouse et al., 2010) The effect of aerosol emissions on cloud formation remains subject to some debate, with a modelling study (Browse et al., 2014) suggesting only weak CCN response to Arctic organic aerosol flux. Nevertheless, direct observations have demonstrated a link between sea surface DMS emissions and particle formation events in the Arctic atmosphere (Chang et al., 2011; Mungall et al., 2016), motivating further quantification of marine DMS emissions in Arctic regions.

To date, logistical constraints have limited the measurements of surface water properties in many high latitude regions, and these areas remain relatively sparsely sampled for DMS/P concentrations. Indeed, of the approximately 50,000 data points in the global Pacific Marine Environmental Laboratory (PMEL) database of oceanic DMS measurements (http://saga.pmel.noaa.gov/dms/), only 5% have been made in either Arctic or Antarctic waters (~ 1600 and 1000 data points, respectively). Despite the relatively limited sulfur observations in high latitude waters, an examination of the available data reveals large differences in the water column DMS distributions of the Arctic and Antarctic regions. While the summertime mean DMS concentration in the Arctic Ocean is 3.0 nM (close to the global mean value of 4.2 nM, derived from the PMEL data), the mean summertime DMS concentration in the Southern Ocean is ~ 3 times higher at 9.3 nM. Moreover, several areas of extraordinarily high DMS concentrations (>100 nM) have been observed in various regions of the Southern Ocean (DiTullio et al. 2000; Tortell et al. 2011), whereas no study to date has observed DMS concentrations above 25 nM in Arctic waters. The available data thus suggest contrasting dynamics of DMS/P production in the two polar regions (i.e. Arctic vs. Antarctic).

Although Arctic and Antarctic regions share several key physical characteristics, most notably strong seasonal cycles in sea ice cover and solar irradiance, there are some critical differences. Much of the pelagic Southern Ocean is an iron-limited, High Nutrient Low Chlorophyll (HNLC) regime, with large seasonal changes in mixed layer depths (MLD) (Boyd et al., 2001). Low iron conditions, and seasonally-variable mixed layer light levels may induce oxidative stress (particularly in ice-influenced stratified

waters) and thus promote high DMS production (Sunda et al., 2002). In addition, parts of the Southern Ocean are characterized by extremely high biomass of *Phaeocystis antarctica* (Smith et al., 2000), a colonial haptophyte that is a prodigious producer of DMSP and DMS (Stefels et al., 2007). By comparison, the salinity-stratified surface waters of the Arctic Ocean are believed to be primarily limited by macronutrient (i.e. nitrate) availability (Tremblay et al., 2006), with a maximum phytoplankton biomass that is at least an order of magnitude lower than that observed in the Southern Ocean (Carr et al., 2006). Despite the relatively low phytoplankton biomass over much of the Arctic Ocean, reasonably high summertime DMS levels (max ~ 25 nM) have been observed in some regions. It is also important to note that significant Arctic phytoplankton biomass and primary productivity may occur in sub-surface layers (Martin et al., 2010), and in under-ice blooms (Arrigo et al., 2012). The quantitative significance of these blooms for DMS production is unknown at present (Galindo et al., 2014).

Quantifying the spatial and temporal distribution of DMS and DMSP in the Arctic Ocean is particularly important in light of the rapidly changing hydrographic conditions across this region. Rapid Arctic warming over the past several decades has been associated with a significant reduction in summer sea ice extent, resulting in higher mixed layer irradiance levels and a longer phytoplankton growing season (Arrigo et al., 2008). Arrigo et al. (2008) suggested that continued warming and sea-ice loss could lead to a three-fold increase in primary productivity over the coming decades. The effects of these potential changes on DMS/P concentrations and cycling remain unknown, but it has been suggested that future changes in Arctic Ocean DMS emissions could modulate

123 regional climatic patterns (Levasseur, 2013). Indeed, modeling work has suggested that
124 cooling associated with increased DMS production and emissions in less ice-covered
125 polar regions may help offset warming associated with loss of sea-ice albedo (Gabric et
126 al., 2004; Cameron-Smith et al., 2011). The important climatic and biological roles of
127 reduced sulfur compounds, combined with altered marine conditions under a warming
128 environment, provide the motivation for a deeper understanding of the distribution and
129 cycling of DMS and related compounds in Arctic waters.

130 In this article, we present a new data set of DMS and DMSP concentrations in
131 Arctic and Subarctic waters adjacent to the Canadian continental shelf. We used a
132 number of recent and emerging methodological approaches to measure these compounds
133 in a continuous ship-board fashion. In particular, we used membrane inlet mass
134 spectrometry (MIMS) to measure DMS with extremely high spatial resolution (i.e. sub-
135 km scale), and the recently developed organic sulfur sequential chemical analysis robot
136 (OSSCAR), for automated analysis of DMS and DMSP. Our goal was to utilize the
137 sampling capacities of the MIMS and OSSCAR systems to make simultaneous
138 measurements of DMS/P in Subarctic Atlantic and Arctic waters, in order to expand the
139 spatial coverage of the existing DMS/P dataset, and identify environmental conditions
140 leading to spatial variability in the concentrations of these compounds.

141 **2. Methods**

142 **2.1 Study Area**

143 Our field study was carried out on board the *CCGS Amundsen* during Leg 2 of the 2015
144 GEOTRACES expedition to the Canadian Arctic, from July10 to August 20, 2015. We

sampled along a ~ 10,000 km transect from Quebec City, Quebec, to Kugluktuk, Nunavut. Data collection commenced off the coast of Newfoundland, and included waters of the Labrador Sea, Baffin Bay and the Canadian Arctic Archipelago (Figure 1).

The cruise transect covered two main distinct geographic domains – the Baffin Bay/Labrador Sea region, and the Canadian Arctic Archipelago (CAA). The majority of the surface water in the CAA is from Pacific-sourced water masses, as a shallow sill near Resolute restricts the westward flow of Atlantic-sourced water (Michel et al., 2006). Flow paths through the CAA are complex. The region is characterized by a network of shallow, narrow straits that are subject to significant regional variability in local mixing and tidal processes, and strongly influenced by riverine input, which drives stratification (Carmack et al, 2011). In contrast, both Atlantic- and Pacific-sourced waters mix in the Baffin Bay and Labrador Sea regions, and this confluence drives a strong thermohaline front, leading to lower stratification than in the CAA (Carmack et al., 2011).

**2.2 Underway sampling systems**

We utilized two complementary underway sampling systems to measure reduced sulfur compounds; MIMS (Tortell, 2005), and OSSCAR (Asher et al., 2015). Detailed methodological descriptions of these systems have been published elsewhere ((Tortell, 2005, 2011), (Asher et al., 2015), and only a brief overview is given here.

**2.2.1 OSSCAR**

The OSSCAR instrument consists of an automated liquid handling / wet chemistry module that is interfaced to a custom-built purge-and-trap gas chromatograph (GC) equipped with a pulsed flame photometric detector (PFPD) for sulfur analysis. A

custom LabVIEW program is used to automate all aspects of the sample handling and data acquisition. During analysis, unfiltered seawater (3 - 5 ml) from an underway supply (nominal sampling depth ~ 5 m) is drawn via automated syringe pump into a sparging chamber. DMS is then stripped out of solution (4 minutes of 50 ml $min^{-1}$ $N_2$ flow) onto a 1/8" stainless steel trap packed with carbopack at room temperature. Rapid electrical heating of the trap (to ~260°C), causes DMS desorption onto a capillary column (Restek SS MXT, 15m, 80 °C, 2 ml $min^{-1}$ $N_2$ flow) prior to detection by the PFPD (OI Analytical, Model 5380). Light emitted during combustion in the PFPD is converted to a voltage and recorded by a custom built Labview data acquisition interface. Following the completion of DMS analysis, 5 M sodium hydroxide is added to the sparging chamber for 14 minutes to cleave DMSP in solution to DMS, following the method of Dacey and Blough (Dacey and Blough, 1987). The resulting DMS is sparged out of solution and measured as described above. The sparging chamber is then thoroughly rinsed with Milli-Q water, and the process can be repeated. As we used unfiltered seawater for our analysis, it is important to note that we measured total DMSP ($DMSP_t$) concentrations, which represent the sum of dissolved and particulate pools.

We measured an in-line standard (20 nM) every 4-5 samples (at most every 3 hours) to ensure that the system was functioning correctly, and to correct for potential detector drift. The mean standard error of daily point standards was 0.55 nM, and we consider this to represent the precision of our emerging method (significant efforts are underway to increase this precision). To correct the underway data for instrument drift, point standard measurements were smoothed with a 3-pt running mean filter, interpolated

to the time-points of sample measurements, and compared to the known standard concentration to provide a drift correction factor for every seawater data point. Six-point calibration curves were performed every two days, using DMS standards (ranging from 0 to 18nM), produced from automated dilutions of a primary DMS stock and Milli-Q water (see Asher et al., 2015). The limit of detection of the system was calculated from the calibration curve using the formula $C_{LOD} = 3s_{y/x} \div b$, where $C_{LOD}$ is the concentration limit of detection, $s_{y/x}$ is the standard error of the regression , and b is the slope of the regression line. With this approach, we derived a mean limit of detection of 1.4 nM. The mean linear calibration curve $R^2$ value, taken over all calibration curves, was 0.9887.

The OSSCAR system is designed to automate the collection of seawater for sequential analysis of DMS, DMSO, and DMSP in a single sample. During our cruise, however, we experienced problems with the DMSO reductase enzyme used to convert DMSO to DMS for analysis, and we therefore configured the instrument to run only DMS and DMSP at sea, with one cycle requiring roughly 30 minutes. We experienced general technical difficulties with the instrument during the early phases of the cruise, and no OSSCAR data are thus available for the first half of the transect.

**2.2.2 MIMS**

We used MIMS to obtain very high frequency measurements (~ several data points per minute) of DMS concentrations and other gases in surface seawater. Using this system, seawater from the ship's underway loop was pumped through a flow-through sampling cuvette, attached, via a silicone membrane, to a quadrupole mass spectrometer (Hiden Analytical HPR-40). DMS was measured by detecting ions with a mass to charge ratio of

62 (m/z 62) every ~30 seconds. To achieve constant sample temperature prior to contact with the membrane, seawater was passed through a 20 foot coil of stainless steel tubing immersed in water bath held at 4 °C (Tortell et al., 2011). The system pressure (as measured by the Penning Gauge) remained stable during operation (~1.3 – 1.5×$10^{-6}$ Torr). The DMS signal was calibrated using liquid standards that were produced by equilibrating 0.2 µm filtered seawater with a constant supply of DMS (m/z 62) from a calibrated permeation device (VICI Metronics). The primary effluent from the permeation tube (held at 30 ± 0.1 °C in a custom-built oven) was split among several capillary outflows and mixed into a $N_2$ stream controlled at 50 ml $min^{-1}$ using a pressure regulator and fixed length / diameter tubing. This system enabled us to achieve a range of DMS / $N_2$ mixing ratios that were bubbled into standard bottles held in an incubator tank supplied with continuously flowing seawater. Concentrations of DMS in the standard bottles were cross-validated by measuring discrete samples using the OSSCAR system. The limit of reliable detection of the MIMS is ~ 2nM (Tortell, 2005).

**2.3 Post-processing of DMS data**

Raw data outputs (voltages) for both OSSCAR and MIMS measurements were processed into final concentrations using MATLAB scripts. For OSSCAR data, raw voltages were captured with a sampling frequency of 5 Hz. Sulfur peaks eluting off the GC column were integrated using a custom MATLAB script, with correction for baseline signal intensities. DMS concentrations were derived from peak areas using the calibration curves as described above.

**2.4 Ancillary seawater data**

233 Shipboard salinity, temperature, wind speed, and chlorophyll *a* (chl *a*)
234 fluorescence measurements were collected using several underway instruments. We used
235 a Seabird Electronics thermosalinograph (SBE 45) for continuous surface temperature
236 and salinity measurements, and a Wetlabs Fluorometer (WetStar) to measure chl *a*
237 fluorescence, as a proxy for phytoplankton biomass. We note that the chl *a* fluorescence
238 data are subject to significant diel cycles associated with light-dependent fluorescence
239 quenching. All sensors were calibrated prior to and following the summer expedition.
240 Conductivity Temperature Depth (CTD) profiles were used to measure vertical profiles of
241 salinity and potential temperature at 17 stations, from which we computed density using
242 the Seawater Toolbox in MATLAB. The mixed layer depth (MLD) was defined as the
243 depth where density exceeded surface values by 0.125 kg $m^{-3}$. Sea ice concentrations
244 were obtained from the AMSR-E satellite product (Cavelieri et al., 2006) with a spatial
245 resolution of 12.5 km. The percent ice cover along the cruise track was derived from a
246 two dimensional interpolation of the ship's position in time and space against the daily
247 sea ice data.
248 All correlation analyses (Pearson's *r*) were computed in MATLAB, using the
249 corrcoef function. Sample sizes were as follows: 33,250 data points in the MIMS DMS
250 dataset, 344 in the OSSCAR DMS dataset, and 318 in the OSSCAR DMSP dataset.
251 **2.5 Phytoplankton biomass and taxonomic composition**
252 In addition to underway data, samples for the quantification of photosynthetic and
253 accessory pigments (Table 1) were collected at a number of discrete oceanographic
254 stations (see Table 2). For each station, duplicate samples (250-500 mL) for chl *a* analysis

were filtered onto pre-combusted 25 mm glass fiber filters (Whatman GF/F) using low vacuum pressure (<100 mm Hg). Filters were stored at -20 ºC and chl *a* was determined within a few days of sample collection using fluorimetric analysis following the method of Welschmeyer (Welschmeyer 1994). Duplicate 1-2 L samples were filtered onto pre-combusted 25 mm GF/F for pigment analysis by reverse-phase High-Performance Liquid Chromatography (HPLC). Filters were dried with absorbent paper, flash frozen in liquid nitrogen and stored at -80 ºC until analysis following the method of Pinckney et al. (1994). We used several diagnostic pigments as markers for individual phytoplankton groups, as described by Coupel et al (2015) (see Table 1). Following HPLC pigment processing, data were interpreted with the chemotaxonomy program CHEMTAX V1.95, using the pigment ratio matrix described by Taylor et al. (2013).

**2.6 DMS Sea-Air Flux**

We derived sea-air fluxes of DMS from MIMS measurements of DMS concentrations, as these data had higher resolution and spatial coverage than OSSCAR observations. We computed sea-air flux as:

$$F_{DMS} = k_{DMS} (DMS_{SW}) (1 - A)^{0.4} \quad (1)$$

where $DMS_{sw}$ is the concentration of DMS in the surface ocean (surface atmospheric DMS is assumed to be zero) and $k_{DMS}$ is the gas transfer velocity derived from the equations of Nightingale et al. (2000), normalized to the temperature and salinity-dependent DMS Schmidt number of Saltzman et al. (1993). The term A represents the proportion of sea ice cover, and the scaling exponent of 0.4 accounts for the effects of sea ice on gas exchange and is derived from the laboratory work of Loose et al. (2009). (We

note that this scaling does not capture all processes present in sea-ice dominated regimes, such as turbulence generated by sea ice melt.) Sea surface salinity and temperature measurements described in section 2.5 were used in the calculations. Wind speed data were obtained from the ship's anemometer (AAVOS data, Environment Canada), corrected to a height of 10 m above the sea surface.

## 3. Results

### 3.1 Oceanographic setting

Figures 1 and 2 show the distribution of hydrographic properties across our cruise survey region. Over our sampling area, surface water temperatures varied between -1.2 and 10.2 °C, while surface salinity ranged from 10.7 to 34.7 psu (Figure 1). The warmest and most saline waters were found in the Labrador Sea, with cold fresher waters in Hudson Strait and the Canadian Arctic Archipelago. Underway chl *a* fluorescence varied between 0.04 and 2.96 μg $L^{-1}$, averaging 0.20 μg $L^{-1}$. The highest chl *a* fluorescence was observed in a localized region within Baffin Bay, in the vicinity of a sharp temperature and salinity frontal zone (Figure 1). Mixed layer depth (MLD) ranged from ~ 5 - 50 m, and were deepest in the Labrador Sea and shallowest in the stations of the Canadian Arctic Archipelago. Sea ice cover was variable across the survey transect, with ice-free waters in the Labrador Sea, and significant ice cover in the northern Hudson Bay and parts of the Canadian Arctic Archipelago (Figure 2).

### 3.2 Phytoplankton biomass and taxonomic distributions

Using measurements of accessory photosynthetic pigments, we examined spatial patterns in the taxonomic composition of phytoplankton assemblages (see Table 1 for a

299 description of HPLC marker pigments and their associated phytoplankton taxa).The
300 distribution of pigments across our sampling stations is presented in Table 2, along with
301 measurements of mixed layer depth and ice cover, while CHEMTAX-derived assemblage
302 estimates are shown in Table 3. In order to remove large potential differences in total
303 phytoplankton biomass, we normalized pigment concentrations to total chl a
304 concentrations measured using HPLC (see Methods, section 2.5).
305 CHEMTAX pigment analysis shows that all stations in the study area were diatom-
306 dominated, although haptophyte, dinoflagellate, and prasinophyte markers were detected
307 in varying quantities at all stations (see Table 3). Total HPLC-measured chl *a* was
308 relatively low throughout the study area, ranging from 0.11 to 0.56 μg $L^{-1}$.
309 **3.3 Observed DMS/P concentration ranges**
310 The DMS data shown in Figure 1 are derived from MIMS measurements, since
311 these have wider geographic coverage and greater spatial resolution than OSSCAR data.
312 DMS concentrations measured with MIMS ranged from 0.2 nM to 12 nM, averaging 2.7
313 (± 1.5) nM. The highest values were observed in the northern Labrador Sea, Baffin Bay
314 and Hudson Strait, with lower values through much of the Arctic Archipelago.
315 Figure 3 shows the distribution of DMS, measured by both MIMS and OSSCAR,
316 along the cruise track. DMS concentrations measured with OSSCAR ranged from 0.1 to
317 18 nM, averaging 3.2 ± 2.4 nM. As described in the discussion, 22% of our derived DMS
318 concentrations fell below the limit of detection. In general, we observed reasonably good
319 coherence between DMS measurements made by our two analytical systems, with similar
320 absolute values of data and spatial patterns. There were, however, notable offsets in the

early August measurements (~ km 7000 cruise track, Figure 3a), when OSSCAR DMS data were consistently higher than MIMS data. Notwithstanding this offset (for which potential reasons are addressed in the discussion), the coherent spatial patterns in data derived from these independent methods is encouraging, particularly given the rather low precision of our current OSSCAR system.

The spatial distribution of DMSP concentrations (measured with OSSCAR) along the cruise track is also shown in Figure 3. Concentrations ranged from <1 nM to 160 nM, and averaged 30 ± 29 nM. DMSP:chl *a* ratios measured from HPLC chl *a* data ranged from 52.31 nmol $\mu g^{-1}$ to 181.4 nmol $\mu g^{-1}$. Examination of the data in Figure 3 reveals that high DMS concentrations were sometimes, but not always, accompanied by high DMSP concentrations. For example, a sharp increase in measured DMSP concentrations (around 7000-7400 km) on the cruise track was accompanied by a sharp increase in DMS measured by both instruments, while low-DMS waters observed around km 9400 along the transect also showed very little DMSP. Over the portion of the transect where measurements of both DMS and DMSP were available, the OSSCAR-measured concentrations of these compounds exhibited a statistically significant positive correlation ($r = 0.52$, $p < 0.001$). There were, however, a number of regions where increased DMS concentrations were not accompanied by increases in DMSP (e.g. ~ km 10,000).

**3.4 Sea-Air Flux**

Figure 4 shows DMS sea-air fluxes as computed from MIMS-measured DMS seawater concentrations, wind speed and sea ice cover. DMS sea-air fluxes ranged from < 1 to 80

343 μmol S $m^{-2}$ $day^{-1}$, with peak sea-air flux calculated around km 5500 on the cruise track.
344 Sea-air flux is highly dependent on wind speed and sea ice cover, with the result that even
345 high concentrations of seawater DMS yielded low sea-air flux when low wind and/or
346 high sea ice was present (e.g. km 2100, 7200, 8300). Conversely, very high sea-air fluxes
347 were observed when moderately high DMS concentrations coincided with high wind
348 speeds and ice-free waters (e.g. km 5400).

349 **3.5 Comparison of gradients in DMS data with hydrographic features**

350 The high sampling frequency of MIMS measurements allows the comparison of
351 DMS observations with other underway environmental variables, and enables the
352 quantification of small-scale DMS concentration gradients in near real-time. Figure 2
353 shows a cruise track record of MIMS-measured DMS concentrations in relation to
354 salinity, temperature, chl *a* fluorescence, and ice cover. Several sharp increases in DMS at
355 around kms 2100, 3300, and 3800 along the cruise track were accompanied by strong
356 gradients in temperature and, to a lesser extent, salinity (Figure 2). These regions
357 correspond to areas in the Labrador Sea and Baffin Bay. An increase in DMS
358 concentrations in Baffin Bay around km 7200 in the cruise track (Figure 2a) was
359 associated with a simultaneous drop in sea-surface temperature and salinity, in close
360 proximity to a sharp increase in chl *a* fluorescence along the cruise track (Figure 2c) (see
361 Figure 1). As shown in Figure 3b, this localized region exhibited the highest
362 concentrations of DMSP along the transect. Interestingly, this area was also characterized
363 by strong gradients in sea ice concentrations, and the low salinity waters are indicative of
364 localized ice melt. Figures 1d and 2d also show the large-scale salinity gradients in the

Hudson Bay and the Canadian Arctic Archipelago, highlighting the freshwater influx in these near-shore areas. In contrast to our observations in Baffin Bay, DMS concentrations showed relatively little variability across these salinity gradients.

In order to more closely examine small-scale variability in DMS and other surface water variables, we calculated spatial gradients in the data to examine the coherence of frontal features in DMS, salinity, temperature and chl *a* fluorescence. For this analysis, we computed gradients in each oceanographic variable within a neighborhood of 100 points surrounding each point. Gradients (G) for each variable (DMS, SST, chl *a*, and salinity) were calculated at each point x as follows:

$$G_x = \frac{V_{x+50} - V_{x-50}}{D_{x+50} - D_{x-50}} \quad (2)$$

Here, G is gradient (in units of change per km), V is the value of the variable at a point, x, and D is the cruise track distance at x. A neighborhood of 100 points, corresponding to a distance of ~25 km, was subjectively chosen because it best captured the observed variability in the data, representing an intermediate value between a localized neighborhood (e.g. 10 points), which would only consider changes close to the point, and a large neighborhood (e.g. 1000 points), which would smooth the features. The results of this analysis (Figure 5) qualitatively demonstrate a coherence of DMS gradients with salinity, chlorophyll, and sea surface temperature.

**3.6 Correlation with ancillary oceanographic variables**

We computed Pearson correlation coefficients of DMS and DMSP with underway measurements of salinity, sea surface temperature, chl *a* fluorescence, and sea ice cover. We also examined the potential relationships between DMS concentrations and MIMS-

derived $pCO_2$, and $\Delta O_2/Ar$ (Tortell et al., in preparation). The results can be seen in Table 4. Only correlations significant at the 0.05 level are included. Only weak correlations are seen between MIMS-measured DMS data and ancillary variables, and OSSCAR DMS data did not exhibit any significant correlations with any ancillary variables, including measured of phytoplankton taxonomic distributions. A significant positive correlation ($r$ = 0.66, $p$<0.001) was found between DMSP and underway chl *a* fluorescence. Over the whole transect, we observed a weak negative correlation between DMS/P and sea-ice cover ($r$ = -0.26 for DMS, and $r$=-0.34 for DMSP, $p$< 0.001 in both cases). A weak positive correlation was found between DMSP/chl *a* and ice cover ($r$ = 0.52, $p$< 0.04), suggesting potential roles for sea-ice microalgae in DMSP production at the sampled stations. It is interesting to note that elevated chl *a* fluorescence and DMSP concentrations often occurred in areas of intermediate ice cover (km 3300, 7300 and 9200 along the cruise track), potentially reflecting the influence of ice-edge blooms or under-ice phytoplankton assemblages. Potential mechanisms for these features are addressed in the discussion.

## 4. Discussion

Our results provide a new dataset of reduced sulfur compounds in an under-sampled region of the Arctic Ocean, enabling an examination of DMS/P variability in relation to various oceanographic properties on a range of spatial scales. Below, we focus our discussion on the observed relationship between gradients in DMS and other oceanographic variables, and discuss the comparability of the two DMS measurement methods utilized. We compare our results to previously published measurements in the

409 Arctic, situating our results in the context of the changing hydrography and
410 phytoplankton ecology of the Arctic Ocean.

411 **4.1 Comparability of MIMS and OSSCAR measurements**

412 The OSSCAR and MIMS instruments have previously shown good agreement in
413 measured DMS concentrations in the Subarctic Pacific Ocean (Asher et al., 2015).
414 Similarly, we observed relatively good coherence between the two methods (Figure 3)
415 over much of our cruise track. The largest exception to this occurred around km 7000,
416 when DMS measurements measured by OSSCAR were significantly higher than those
417 measured by MIMS. This region was characterized by very high DMSP measurements
418 (often one order of magnitude higher than the DMS measurements). If small amounts of
419 DMS remained in the OSSCAR system after DMSP analysis, sample carry-over could
420 contribute to higher measured concentrations in the subsequent DMS analysis. In order
421 to minimize this potential artifact, the system was thoroughly rinsed with MilliQ water
422 after every run. The effectiveness of this rinse was tested by subsequently purging DMSP
423 standards without NaOH, and no carryover was observed. It is possible, however, that
424 this approach was not entirely efficient. Another potential cause of the higher OSSCAR
425 DMS measurements may be due to cell breakage during the sparging process in
426 OSSCAR. In this scenario, there is the potential for release of intracellular DMSP and
427 DMSP lyase into solution, which would lead to artificially high measured DMS
428 concentrations. It is not possible for us to quantify the magnitude of such a potential
429 artefact, but we note that its magnitude would likely depend on the taxonomic
430 composition of phytoplankton assemblages. Wolfe et al. (2002) showed that sample

sparging led to an increase in DMS production by both the haptophyte *Emiliana huxleii* and the dinoflagellate *Alexandrium*. Unfortunately, due to limited coverage of discrete sampling, we do not have any estimates of phytoplankton community composition in the region where MIMS and OSSCAR showed the greatest discrepancies. Notwithstanding these potential caveats, we suggest that the two methods show strong promise to provide complementary information on DMS/P (and DMSO) concentrations in surface ocean waters.

One challenge going forward is to increase the reproducibility and sensitivity of OSSCAR measurements, and this is an area of active work in our group. The version of our system used in 2015 had a detection limit of roughly 1.4 nM, and was thus far less sensitive than many conventional GC methods, which can achieve sub-nM detection limits. Our detection limit was of only minor consequence for DMSP measurements, given that 72% of measured DMSP concentrations were higher than 10 nM, and less than 3% fell below 1.4 nM. The relatively low sensitivity was somewhat more problematic for DMS, with approximately 22% of our OSSCAR-measured DMS values below 1.4 nM. Nonetheless, as discussed below, we believe that the OSSCAR data, in combination with our MIMS data, provide useful information on the spatial distribution of both DMSP and DMS in Arctic waters.

**4.2 Towards a regional Arctic data base of DMS/P concentrations**

Figure 6 shows a comparison between our Arctic DMS measurements (made by OSSCAR) and other summertime Arctic DMS data in the PMEL database. For this comparison, only PMEL measurements made above the Arctic circle (66.56° N) in June-

453 August are included, resulting in a total of 415 data points. As shown in Figure 6, the
454 majority of available summertime PMEL DMS/P measurements are found in the Atlantic
455 region of the Arctic, and in the Bering Sea, with limited data in the Canadian Archipelago
456 (for an overview of Arctic DMS/P studies performed to date, see Levasseur, 2013). For
457 the sake of visual clarity, the presentation of data in Figure 6a is based on DMS
458 measurements made by OSSCAR, whereas both sets of data were included in the
459 frequency distribution analysis (Figure 6b). The results presented in Figure 6 suggest that
460 our measurements are representative of the broader Arctic context, with generally similar
461 data frequency distributions (Figure 6b) for all three DMS datasets (MIMS, OSSCAR,
462 and PMEL). From the map, we see that the spatial footprint of our measurements
463 complement the existing summer data, helping to expand the spatial coverage of DMS
464 observations in the Arctic Ocean.
465 In addition to complementing the existing PMEL DMS database, our new
466 observations also build on a number of other reduced sulfur measurements in the
467 Canadian Sector of the Arctic Ocean. Observations of DMS and DMSP derived from
468 several past Arctic and subarctic Atlantic surveys are summarized in Table 5. This table
469 focuses mainly on DMS and DMSP measurements made in the Canadian sector and
470 Greenland waters, serving to provide context for our measurements performed in similar
471 environments. The data presented in Table 5 are obtained from different times of year,
472 and from phytoplankton assemblages of varying taxonomic composition, allowing us to
473 examine DMS and DMSP concentrations in surface waters under a range of
474 environmental and ecological conditions. For example, Bouillon et al. (2002) observed

low DMS concentrations (<1 nM) during a large spring diatom bloom (~ 15 μg $L^{-1}$chl *a*) in the North Water region. In contrast, higher DMS concentrations have been reported later in the season when total phytoplankton biomass is lower, and taxonomic composition has shifted away from diatom-dominance. Working in the same geographic region as Bouillon, Motard-Côté et al. (2012) reported higher late summer (September) DMS levels (maximum = 4.8 nM), which were accompanied by moderate chl *a* concentrations (0.2-1 μg $L^{-1}$ ), while Luce et al. (2011) reported very low DMS (<1 nM) associated with moderate chl *a* concentrations (0.2-2 μg$L^{-1}$) in a flagellate dominated community in late fall (October-November), with DMS decreasing towards the later months. A similar pattern was observed in the northwest subarctic Atlantic by Lizotte et al. (2012), who associated elevated reduced sulphur (DMSP) production with flagellate and prymnesiophyte communities in midsummer and fall, in contrast to early-season diatom blooms with little associated DMSP and DMS. This seasonal decrease in DMS levels may be potentially attributable to light limited primary productivity, and diminishing capacity for light-induced oxidative stress, which has been shown to increase DMS/P production (Sunda et al., 2002).

To date, the highest recorded Arctic water column measurements of DMS (25 nM) and DMSP (160 nM) have been observed during mid-summer blooms of the haptophyte *Phaeocystis* at the ice edge (see Matrai and Vernet, 1997; Gali and Simo, 2010). Our mid-season (July-August) study of similar areas shows moderately high DMS (up to 18 nM) accompanied by relatively low chl *a* (0.11- 1.06 μg $L^{-1}$) in a mixed community where flagellates and prasinophytes are present.

Together, the available data (Table 5 and our measurements) are consistent with a seasonal cycle in Arctic and subarctic reduced sulfur distributions. Early season diatom-dominated blooms exhibit high biomass and primary productivity but low DMS/P accumulation, while mid-summer phytoplankton assemblages dominated by haptophytes and dinoflagellates display lower phytoplankton biomass but higher reduced sulfur accumulation. This pattern is similar to the summertime 'DMS paradox' reported in a number of temperate and sub-tropical waters (Simo and Pedrós-Alió, 1999). In the fall, both Arctic primary productivity and DMS/P production decrease with the onset of lower temperatures and increased ice cover. Our data are consistent with this general scenario, representing a mixed-species assemblage with moderate biomass and DMS/P accumulation.

**4.3 Gradients in DMS and hydrographic frontal structures**

The high resolution afforded by the MIMS dataset allows for the observation of fine-scale variability in DMS concentrations at the sub-kilometer scale. Previous studies (Tortell, 2005; Tortell et al., 2011) have quantified fine-scale variability in DMS concentrations, demonstrating de-correlation length scales on the order of 10s of Km, and often shorter than that of other oceanographic variables such as temperature and salinity. These length-scales provide information on the spatial scale of processes driving the majority of variability in DMS concentrations. Figures 2 and 5 clearly demonstrate that gradients in DMS and chl *a* fluorescence often co-occur with strong gradients in temperature and salinity. This suggests a potential role for hydrographic fronts in driving changes in DMS concentrations. Several potential mechanisms may explain this

519 phenomenon. For example, the frontal mixing of distinct water masses, driven by
520 currents, wind, or melting ice, may introduce nutrients into a low-nutrient water column,
521 stimulating localized primary productivity (Tremblay et al. (2011) and potentially
522 increasing DMS/P production. Note that this localized increase in productivity and
523 potential DMS/P production would operate independently of the overall seasonal
524 progression towards increased DMS/P production during the latter summer growth
525 season. Mixing of water masses may also potentially expose water column phytoplankton
526 to light shock or osmotic stress by mixing them upwards in the water column or
527 introducing an abrupt salinity gradient. Both of these factors could contribute to elevated
528 DMSP production, given its hypothesized role as an intracellular osmolyte and anti-
529 oxidant (Stefels et al., 2007). Although our data do not allow mechanistic interpretation
530 for the underlying causes of DMS variability in surface waters, the high resolution
531 afforded by MIMS measurements enables real-time observations of DMS gradients,
532 which may be useful in the design of future process studies examining the driving forces
533 for elevated DMS accumulation.
534
535 **4.4 Influence of phytoplankton assemblage composition and mixed layer depth**
536 Previous work has addressed the role of phytoplankton taxonomic composition
537 and irradiance levels (Stefels et al., 2007) in driving the cycling of DMS/P in marine
538 waters. Here we discuss the potential influence of these factors across our survey region.
539 The majority of the sampled stations were characterized by very shallow mixed layer
540 depths (MLD; Table 2) resulting from strong salinity-based stratification of surface

541 waters. Light stress associated with shallow MLD may contribute to elevated DMSP : chl
542 *a* ratios, and previous studies (Vallina, 2007) have shown high correlation between solar
543 irradiance and surface DMS concentrations. In our dataset, however, there was no
544 overall correlation between MLD and DMSP : Chl ratios. We did, however, observe
545 elevated DMSP concentrations at two stations (BB3 and CAA6) with shallow MLDs.
546 The elevated DMSP : chl *a* ratios measured in our study may also reflect the
547 presence of high-DMSP producing taxa, a phenomenon previously reported by other
548 groups (Matrai et al., 1997; Gali et al., 2010; Lizotte et al., 2012). When comparing our
549 DMSP: chl *a* ratios to other measurements, it is important to note that we measured
550 $DMSP_t$, while many other groups present $DMSP_p$, without taking into account the
551 dissolved fraction ($DMSP_d$). As the dissolved DMSP pool typically makes up a small
552 (though highly variable) portion of the total water column DMSP pool, the use of DMSPt
553 does not likely have a large effect on derived DMSP:chl *a* ratios (Kiene et al., 2000;
554 2006). Despite the potential caveats raised above, the $DMSP_t$:chl *a* ratios we measured
555 across our sampling stations (52-182 nmol $\mu g^{-1}$) were broadly similar to $DMSP_p$:chl *a*
556 values found by Motard-Côté et al. (15-229 nmol $\mu g^{-1}$) in the same region in September
557 (Motard-Côté et al., 2011). In contrast, our measured $DMSP_t$:chl *a* ratios are significantly
558 higher than those measured by Luce et al. (maximum of 39 nmol $\mu g^{-1}$) (Luce et al., 2007)
559 and Matrai and Vernet (maximum 17 nmol $\mu g^{-1}$) at diatom-dominated stations in the
560 Barents Sea (Matrai and Vernet., 1997). The higher DMSP : Chl ratios we measured may
561 be attributable to the presence of mixed (rather than diatom-dominated) assemblages
562 present in the study area at the time of sampling. We cannot, however, draw any firm

563 conclusions on the role of taxonomy in controlling DMSP:Chla, as we were unable to
564 detect any significant correlations between DMSP:chl *a* and HPLC pigment markers for
565 different phytoplankton groups.

566 To conclude, our observations do not permit us to establish a firm link between
567 MLD, phytoplankton taxonomy and DMS/P concentrations. Other factors, including
568 bacterial activity and zooplankton grazing are potential contributing factors, but we lack
569 the data needed to examine the importance of these processes.

570 **4.5The interaction of DMS/P and sea ice**

571 The presence of sea ice exerts a strong control on polar phytoplankton by
572 controlling irradiance levels in the water column (Levasseur, 2013), and influencing
573 vertical mixing, stratification and nutrient accumulation. It is thus expected that the
574 presence of sea-ice may affect DMS/P cycling. In a 2010 study, Gali et al. (2010) found
575 that Arctic sea ice melt drove stratification of nutrient rich surface water, triggering a
576 sharp increase in primary productivity, with associated elevated DMS and DMSP levels.
577 These authors also showed that experimental exposure of phytoplankton to high light
578 conditions (mimicking those that would follow the breakup of sea ice) led to near-total
579 release of intracellular DMSP, providing one possible explanation for elevated DMSP
580 levels in the water column. A number of studies also show that the ice, itself, can be a
581 potentially significant reservoir of reduced sulfur, associated with bottom ice-algae
582 (Levasseur et al., (1994).

583 The weak negative correlation we observed between sea ice cover and DMS/P
584 concentration is consistent with the idea that sea ice cover limits insolation, thereby

585 reducing primary productivity and DMS/P production. In general, the drivers of DMSP
586 and DMS production differ – though DMSP production has been shown to be directly
587 influenced by sea ice melt in under-ice blooms (Galindo et al., 2014), the production of
588 DMS from DMSP is largely dependent on the metabolism of in situ bacterial assemblages
589 (Evans et al., 2007), and may therefore be uncoupled from the influence of ice on
590 phytoplankton activity. It is interesting to note, however, that several sharp increases in
591 DMS (observed with MIMS) occurred simultaneously with the occurrence of small
592 amounts of sea ice (<20% total cover) (Figure 2, kms 3400 and 7200 on the cruise track).
593 Limited station data also indicate high DMSP:chl *a* ratios in areas with a comparatively
594 high sea ice cover, at stations BB3 and CAA6 (Table 2). At the time of our sampling,
595 both of these stations were characterized by very low phytoplankton biomass (0.11 μg $L^{-1}$
596 and 0.20 μg $L^{-1}$chl *a*, respectively) and had particularly high DMSP: chl *a* ratios (129
597 nmol $\mu g^{-1}$ and 182 nmol $\mu g^{-1}$, respectively). This suggests a potential role for ice-edge
598 effects, either through the melt-induced stimulation of reduced sulfur production in
599 DMSP rich phytoplankton taxa, or through the release of ice-associated DMSP into the
600 water column. Figures 2d and 2e show decreased salinity in partially ice-covered areas
601 (e.g. around kms 4400, 7300, and 9200), suggesting some melt-water stratification
602 effects. Previous groups have also reported elevated DMS and DMSP concentrations in
603 partially ice-covered water and ice-edge regions in the Arctic Ocean ( Matrai and Vernet,
604 1997; Gali et al. (2010); Leck and Persson 1997).
605
606

## 5. Conclusion

We present a high spatial resolution dataset of reduced sulfur measurements through the Canadian sector of the Arctic Ocean and Subarctic Atlantic. We demonstrate the utility of high-resolution DMS measurements for comparison with other oceanographic variables, and show the coherence of DMS gradients with fine-scale surface hydrographic structure, suggesting elevated DMS production in some oceanographic frontal zones. We also observed elevated DMS/P values in partially ice-covered regions, suggesting that ice-edge effects may stimulate DMS/P production. Our data serve to significantly expand the existing spatial coverage of reduced sulfur measurements in the Arctic, providing a baseline for future studies in this rapidly changing marine environment. Future warming of surface waters and sea-ice melt could lead to increased concentrations and sea-air fluxes of DMS, though significantly more observations will be needed to substantiate this.

**Acknowledgements:** This work was supported by grants from the Natural Sciences and Engineering Research Council of Canada (NSERC) through the Climate Change and Atmospheric Research program (Arctic-GEOTRACES). We are grateful to the captain and crew of the *CCGS Amundsen* for their invaluable support in this work.

**Data Availability:**

All data are available at the following github repository:

**https://github.com/tjarnikova/Jarnikova_Canadian_Arctic_DMS_supldata (DOI: 10.5281/zenodo.160225)**

## References


Arrigo, K.R., van Dijken, G., and Pabi, S.: Impact of a shrinking Arctic ice cover on marine primary production, Geophys. Res. Lett., 35, L19603, doi:10.1029/2008GL035028, 2008.

Arrigo, K.R., Perovich, D.K., Pickart, R.S., and Brown, Z.W.: Massive phytoplankton blooms under Arctic sea ice, Science, 336,1408, doi:10.1126/science.1215065, 2012.

Asher, E., Dacey, J., Jarníková, T., and Tortell, P.: Measurement of DMS, DMSO, and DMSP in natural waters by automated sequential chemical analysis, Limnol. Oceanogr-Meth., 13, 451–462, doi:10.1002/lom3.10039, 2015.

Asher, E., Dacey, J., Stukel, M., Long, M.C., and Tortell, P.: Processes driving seasonal variability in DMS, DMSP, and DMSO concentrations and turnover in coastal Antarctic waters, Limnol. Oceanogr., 62, 104-124, doi: 10.1002/lno.10379, 2016.

Bouillon, R.C., Lee, P.A., de Mora, S.J., and Levasseur., M.: Vernal distribution of dimethylsulphide, dimethylsulphoniopropionate, and dimethylsulphoxide in the North Water in 1998, Deep-Sea Res., 49, 5171-5189, doi:10.1016/S0967-0645(02)00184-4, 2002.

Boyd, P.W., Crossley, A.C., DiTullio, G.R., Griffiths, F.B., Hutchins, D.A., Queguiner, B., Sedwick, P.N. and Trull, T.W.: Control of phytoplankton growth by iron supply and irradiance in the subantarctic Southern Ocean: Experimental results from the

SAZ Project, J. Geophys. Res., 106, 31573–31583, doi:10.1029/2000JC000348, 2001.

Cameron-Smith, P., Elliott, S., Maltrud, M., Erickson, D., and Wingenter, O.: Changes in dimethyl sulfide oceanic distribution due to climate change, Geophys. Res. Lett., 38, L07704, doi:10.1029/2011GL047069.

Carmack, E., and McLaughlin, F.: Towards a recognition of physical and geochemical change in Subarctic and Arctic Seas, Prog. Oceanogr., 90, 90-104, doi: 10.1016/j.pocean.2011.02.007, 2011.

Carr, M.-E., Friedrichs, M.A.M, Schmeltz, M., Aita, M.N., Antoine, D., Arrigo, K.R., Asanuma, I., Aumont, O., Barber, R., Behrenfeld, M. Bidigare, R., Buitenhuis, E.T., Campbell, J., Ciotti, A., Dierssen, H., Dowell, M., Dunne, J., Esaias, W., Gentili, B., Gregg, W., Groom, S., Hoepffner, N., Ishizaka, J., Kameda, T., Le Quéré, C., Lohrenz, S., Mara, J., Mélin, F., Moore, K., Morel, A., Reddy, T., Ryan, J., Scardi, M., Smyth, T., Turpie, K., Tilstone, G., Waters, K., and Yamanaka, Y.: A comparison of global estimates of marine primary production from ocean color, Deep-Sea Res. Pt. II., 53, 741–770, doi:10.1016/j.dsr2.2006.01.028, 2006.

Cavelieri, D.J., Markus, T., Hall, D. K., Gasiewski, A. J., Klein, M., and Ivanoff, A.: Assessment of EOS Aqua AMSR-E Arctic Sea Ice Concentrations Using Landsat-7 and Airborne Microwave Imagery, IEEE T. Geosci. Remote., 44, 3057-3069, doi: 10.1109/TGRS.2006.878445, 2006.

679 Chang, R., Sjostedt, S., Pierce, J., Papakyriakou, T., Scarratt, M., Michaud, S.,
680 Levasseur, M., Leaitch, R., and Abbatt, J.: Relating atmospheric and oceanic DMS
681 levels to particle nucleation events in the Canadian Arctic, J. Geophys. Res., 116,
682 D00S03, doi:10.1029/2011JD015926, 2011.
683
684 Charlson, R., Lovelock, J., Andreae, M., and Warren, S.: Oceanic phytoplankton,
685 atmospheric sulphur, cloud albedo and climate, Nature, 326, 655–661,
686 doi:10.1038/326655a0, 1987.
687
688 Coupel, P., Matsuoka, A., Ruiz-Pino, D., Gosselin, M., Marie, D., Tremblay, J.-É., and
689 Babin, M.: Pigment signatures of phytoplankton communities in the Beaufort Sea,
690 Biogeosciences, 12, 991–1006, doi:10.5194/bg-12-991-2015, 2015.
691
692 Dacey, J., and Blough, N.V.: Hydroxide decomposition of dimethylsulfoniopropionate to
693 form dimethylsulfide, Geophys. Res. Lett., 14, 1246-1249,
694 doi:10.1029/GL014i012p01246, 1987.
695
696 DiTullio, G., Grebmeier, J., Arrigo, K., Lizotte, M., Robinson, D., Leventer, A., Barry, J.,
697 VanWoert, M., and Dunbar, R.: Rapid and early export of Phaeocystis antarctica
698 blooms in the Ross Sea, Antarctica, Nature, 404, 595–598, doi:10.1038/35007061,
699 2000.
700 Evans, C., Kadner, S. V., Darroch, L.J., Wilson, W. H., Liss, P. S., and Malin, G.: The
701 relative significance of viral lysis and microtzooplankton grazing as pathways of
702 dimethylsulfoniopropionate (DMSP) cleavage: An Emiliana huxleyi culture study,
703 Limnol. Oceanogr., 52, 1036-1045, doi: 10.4319/lo.2007.52.3.1036, 2007.

Gabric, A., Simó, R., Cropp, R., Hirst, A., and Dachs, J.: Modeling estimates of the global emission of dimethylsulfide under enhanced greenhouse conditions, Global Biogeochem. Cy., 18, GB2014, doi:10.1029/2003GB002183, 2004.

Galí, M, and Simó, R.: Occurrence and cycling of dimethylated sulfur compounds in the Arctic during summer receding of the ice edge, Mar. Chem., 122, 105-117, doi:10.1016/j.marchem.2010.07.003, 2010.

Galindo, V., Levasseur, M., Mundy, C.J., Gosselin, M., Tremblay, J. -É., Scarratt, M., Gratton, Y., Papakiriakou, T., Poulin, M., and Lizotte, M.: Biological and physical processes influencing sea ice, under-ice algae, and dimethylsulfoniopropionate during spring in the Canadian Arctic Archipelago, J. Geophys. Res-Oceans, 119, 3746–3766, doi:10.1002/2013jc00949, 2014.

Galindo, V., Levasseur, M., Mundy, C.J., Gosselin, M., Scarratt, M., Papakyriakou, T., Stefels, J., Gale, M., Tremblay, J.-É., and Lizotte, M.: Contrasted sensitivity of DMSP production to high light exposure in two Arctic under-ice blooms, J. Exp. Mar. Biol. Ecol., 475, 38–48, doi:10.1016/j.jembe.2015.11.009, 2016.

Keller, M.D.: Dimethyl sulfide production and marine phytoplankton: the importance of species composition and cell size, Biol. Oceanogr., 6, 375-382, doi:10.1080/01965581.1988.10749540, 1989.

Kiene, R., Linn, L. J., and Bruton, J.A.: New and important roles for DMSP in marine microbial communities, J. Sea Res., 43, 209-224, doi: 10.1016/S1385-

730 1101(00)00023-X, 2000.
731
732 Kiene, R.P., and Linn, L.J.: Distribution and turnover of dissolved DMSP and its
733 relationship with bacterial production and dimethylsulfide in the Gulf of Mexico,
734 Limnol. Oceanogr., 45, 849-861, doi:10.4319/lo.2000.45.4.0849, 2000.
735
736 Kiene, R., and Slezak, D.: Low dissolved DMSP concentrations in seawater revealed by
737 small-volume gravity filtration and dialysis sampling, Limnol. Oceanogr.-Meth., 4,
738 80–95, doi:10.4319/lom.2006.4.80, 2006.
739
740 Lana, A., Bell, T.G., Simó, R., Vallina, S.M., Ballabrera-Poy, J., Kettle, A.J., Dachs, J.,
741 Bopp, L., Saltzman, E.S., Stefels, J., Johnson, J.E., and Liss, P.S.: An updated
742 climatology of surface dimethlysulfide concentrations and emission fluxes in the
743 global ocean, Global Biogeochem. Cy., 25, GB1004, doi:10.1029/2010GB003850,
744 2011.
745
746 Leck, C., and Persson, C.: The central Arctic Ocean as a source of dimethyl sulfide
747 Seasonal variability in relation to biological activity, Tellus B, 48B(2), 156–177,
748 doi:10.1034/j.1600-0889.1996.t01-1-00003.x, 1996.
749
750 Levasseur, M., Gosselin, M., and Michaud, S.: A new source of dimethylsulfide (DMS)
751 for the arctic atmosphere: ice diatoms, Mar. Biol., 121, 381–387,
752 doi:10.1007/BF00346748, 1994.
753
754 Levasseur, M., Impact of Arctic meltdown on the microbial cycling of sulphur, Nat.
755 Geosci., 6, 691–700, doi:10.1038/ngeo1910, 2013.

Lizotte, M., Levasseur, M., Michaud, S., Scarratt, M., Merzouk, A., Gosselin, M., Pommier, J., Rivkin, R., and Kiene, R.: Macroscale patterns of the biological cycling of dimethylsulfoniopropionate (DMSP) and dimethylsulfide (DMS) in the Northwest Atlantic, Biogeochemistry, 110, 183–200, doi:10.1007/s10533-011-9698-4, 2012.

Loose, B., McGillis, W.R., and Schlosser, P.: Effects of freezing, growth, and ice cover on gas transport processes in laboratory seawater experiments, Geophys. Res. Lett., 36, L05603, doi:10.1029/2008GL036318, 2009.

Luce, M., Levasseur, M., Scarrat, M.G., Michaud, S., Royer, S.-J., Kiene, R., Lovejoy, C., Gosselin, M., Poulin, M., Gratton, Y., and Lizotte, M.: Distribution and microbial metabolism of dimethylsulfoniopropionate and dimethylsulfide during the 2007 Arctic ice minimum, J. Geophys. Res.-Oceans, 116, C00G06, doi:10.1029/2010JC006914, 2011.

Malin, G., Wilson, W.H., Bratbak, G., Liss, P.S., and Mann, N.H.: Elevated production of dimethylsulfide resulting from viral infection of cultures of Phaeocystis pouchetii, Limnol. Oceanogr., 43, 1389–1393, doi: 10.1016/S0967-0645(02)00184-4, 1998.

Martin, J., Tremblay, J. Gagnon, J., Tremblay, G., Lapoussière, A., Jose, C., Poulin, M., Gosselin, M., Gratton, Y., and Michel, C.: Prevalence, structure and properties of subsurface chlorophyll maxima in Canadian Arctic waters, Mar. Ecol. Prog. Ser., 412, 69–84, doi:10.3354/meps08666, 2010.

782 Matrai, P., and Vernet, M.: Dynamics of the vernal bloom in the marginal ice zone of the
783 Barents Sea: Dimethyl sulfide and dimethylsulfoniopropionate budgets, J. Geophys.
784 Res.-Oceans, 102, 22965-22929, doi:10.1029/96JC03870, 1997.
785
786 Michel, C., Ingram, R. G., and Harris, L. R.: Variability in oceanographic and ecological
787 processes in the Canadian Arctic Archipelago, Prog. Oceanogr., 71, 379–401,
788 doi:10.1016/j.pocean.2006.09.006, 2006.
789
790 Motard-Côté, J., Levasseur, M., Scarratt, M.G., Michaud, S., Gratton, Y., Rivkin, R.B.,
791 Keats, K., Gosselin, M., Tremblay, J.-É., and Kiene, R.P.: Distribution and
792 metabolism of dimethylsulfoniopropionate (DMSP) and phylogenetic affiliation of
793 DMSP-assimilating bacteria in northern Baffin Bay/Lancaster Sound, J. Geophys.
794 Res-Oceans, 117, C00G11, doi:10.1029/2011JC007330, 2012.
795
796 Mungall, E., Croft, B., Lizotte, M., Thomas, J., Murphy, J., Levasseur, M., Martin, R.,
797 Wentzell, J., Liggio, J., and Abbatt, J.: Dimethyl sulfide in the summertime Arctic
798 atmosphere: measurements and source sensitivity simulations, Atmos. Chem. Phys.,
799 16, 6665–6680, doi:10.5194/acp-16-6665-2016, 2016.
800
801 Nightingale, P.D., Malin, G., and Law, C.S.: In situ evaluation of air-sea gas exchange
802 parameterizations using novel conservative and volatile tracers, Global
803 Biogeochem. Cy., 14, 373-387, doi:10.1029/1999GB900091, 2000.
804
805 Pinckney, J., Papa, R., and Zingmark, R.: Comparison of high-performance liquid
806 chromatographic, spectrophotometric, and fluorometric methods for determining

chlorophyll a concentrations in estaurine sediments, Journal of Microbiol. Meth., 19, 59–66, doi:10.1016/0167-7012(94)90026-4, 1994.

Quinn, P.K., and Bates, T.S.: The case against climate regulation via oceanic phytoplankton sulphur emissions, Nature, 480, 51-56, doi: 10.1038/nature10580, 2011.

Saltzman, E.S., King, D.B., Holmen, K., and Leck, C.: Experimental determination of the diffusion coefficient of dimethylsulfide in water, J. Geophys. Res., 98, 16481–16486, doi:10.1029/93JC01858, 1993.

Scarratt, M., Levasseur, M., Michaud, S., and Roy, S.: DMSP and DMS in the Northwest Atlantic: Late-summer distributions, production rates and sea-air fluxes, Aquat. Sci., 69, 292–304, doi:10.1007/s00027-007-0886-1, 2007.

Simó, R., and Pedrós-Alió, C.: Role of vertical mixing in controlling the oceanic production of dimethyl sulphide, Nature, 402, 396–399, doi:10.1038/46516, 1999.

Simó, R.: Production of atmospheric sulfur by oceanic plankton: Biogeochemical, ecological and evolutionary links, *Trends Ecol. Evol.*, **16**, 287–294, doi:10.1016/S0169-5347(01)02152-8, 2001.

Smith, W., Marra, J., Hiscock, M., and Barber, R.: The seasonal cycle of phytoplankton biomass and primary productivity in the Ross Sea, Antarctica, Deep-Sea Res. Pt. II., 47, 3119–3140, doi:10.1016/S0967-0645(00)00061-8, 2000.

Stefels, J., Steinke, M., Turner, S., Malin, G., and Belviso, S.: Environmental constraints on the production and removal of the climatically active gas dimethylsulphide (DMS) and implications for ecosystem modelling, Biogeochemistry, 83, 245–275, doi:10.1007/s10533-007-9091-5, 2007.

Sunda, W., Kieber, D.J., Kiene, R.P., and Huntsman, S.: An antioxidant function for DMSP and DMS in marine algae, Nature, 418, 317–20, doi:10.1038/nature00851, 2002.

Taylor, R. L., Semeniuk, D. M., Payne, C. D., Zhou, J., Tremblay, J., Cullen, J. T., and Maldonado, M. T.: Colimitation by light, nitrate, and iron in the Beaufort Sea in late summer, J. Geophys. Res.-Oceans, 118, 3260–3277, doi:10.1002/jgrc.20244, 2013.

Tortell, P.D., Dissolved gas measurements in oceanic waters made by membrane inlet mass spectrometry, Limnol. Oceanogr.-Meth., 3, 24-37, doi: 10.4319/lom.2005.3.24, 2005.

Tortell, P. D., Guéguen, C., Long, M. C., Payne, C. D., Lee, P., and DiTullio, G. R.: Spatial variability and temporal dynamics of surface water pCO2, ΔO2/Ar and dimethylsulfide in the Ross Sea, Antarctica, Deep-Sea Res. Pt. I., 58, 241–259, doi:10.1016/j.dsr.2010.12.006, 2011.

856 Tremblay, J.E., Michel, C., Hobson, K.A., Gosselin, M., and Price, N.: Bloom dynamics
857 in early opening waters of the Arctic Ocean, Limnol. Oceanogr. 51, pp.900-912.
858 doi: 10.4319/lo.2006.51.2.0900, 2006.
859
860 Tremblay, J., Bélanger, S., and Barber, D.G.: Climate forcing multiplies biological
861 productivity in the coastal Arctic Ocean, Geophys. Res. Lett., 38,
862 doi:10.1029/2011GL048825, 2011.
863
864 Vallina, S.M., and Simó, R.: Strong relationship between DMS and the solar radiation
865 dose over the surface ocean, Science, 315, 506-8. doi: 10.1126/science.1133680
866
867 Welschmeyer, N.A., Fluorometric analysis of chlorophyll a in the presence of chlorophyll
868 b and pheopigments, Limnol. Oceanogr., 39, 1985-1992,
869 doi:10.4319/lo.1994.39.8.1985, 1994.
870
871 Wolfe, G.V., Strom, S.L., Holmes, J.L., Radzio, T. and Olson, M.B.:
872 Dimethylsulfoniopropionate cleavage by marine phytoplankton in response to
873 mechanical, chemical, or dark stress. J. Phycol., 38, 948-960. doi:10.1046/j.1529-
874 8817.2002.t01-1-01100.x, 2002.
875
876 Woodhouse, M.T, Carslaw, K.S., Mann, G.W., Vallina, S.M., Vogt, M., Halloran, P.R.,
877 and Boucher, O.: Low sensitivity of cloud condensation nuclei to changes in the
878 sea-air flux of dimethyl-sulphide, Atmos. Chem. Phys., 10, 7545–7559,
879 doi:10.5194/acp-10-7545-2010, 2010.
880

Zubkov, M.V, Fuchs, B., Archer, S., Kiene, R., Amann, R., and Burkill, P.: Linking the composition of bacterioplankton to rapid turnover of dissolved dimethylsulphoniopropionate in an algal bloom in the North Sea, Environ. Microbiol., 3, 304–311, doi:10.1046/j.1462-2920.2001.00196.x, 200

**Tables**

| Pigment | Associated Taxa |
|---|---|
| **Chlorophyll $c_3$** | Haptophytes |
| **Peridinin** | Dinoflagellates |
| **19'-butanoyloxyfucoxanthin** | Haptophyte |
| **Fucoxanthin** | Diatoms, Haptophytes |
| **19'-hexanoyloxyfucoxanthin** | Haptophytes, Dinoflagellates |
| **Diadinoxanthin** | Haptophytes, Dinoflagellates, Diatoms |
| **Violaxanthin** | Dinoflagellates |
| **Zeaxanthin** | Dinoflagellates |

**Table 1. HPLC marker pigments and their associated phytoplankton taxa. Adapted from Coupel et al. (2015) .**

| Station | Lat(N) | Lon(E) | MLD(m) | % Ice Cover | chl*a* (ug $L^{-1}$) | DMS/ chl*a* (nmol $\mu g^{-1}$) | DMSP/ chl*a* (nmol $\mu g^{-1}$) | Perid/ chl*a* | 19'ButFuc/ chl*a* | Fuc/ chl*a* | 19'HexFuc/ chl*a* | Diadino/ chl*a* |
|---|---|---|---|---|---|---|---|---|---|---|---|---|
| **K1** | 56.12 | -53.37 | 18.4 | *nd* | 0.51 | 6.6 | *nd* | 0.043 | 0.077 | 0.184 | 0.156 | 0.056 |
| **LS2** | 60.45 | -56.55 | 41.4 | *nd* | 0.59 | 3.4 | *nd* | 0.051 | 0.012 | 0.277 | 0.025 | 0.024 |
| **BB3** | 71.41 | -68.59 | 8.2 | 19.7 | 0.12 | *bdl* | 129.4 | 0.049 | 0.011 | 0.278 | 0.051 | 0.087 |
| **BB2** | 72.75 | -67.00 | 10.3 | *nd* | 0.19 | 21.7 | 93.3 | 0.050 | 0.015 | 0.312 | 0.089 | 0.072 |
| **CAA1** | 74.52 | -80.56 | 32.1 | *nd* | 0.56 | 6.9 | 52.3 | 0.015 | 0.018 | 0.239 | 0.023 | 0.042 |
| **CAA5** | 74.12 | -91.49 | 5.3 | 6.61 | 0.16 | *bdl* | 114.7 | 0.078 | 0.017 | 0.326 | 0.020 | 0.051 |
| **CAA6** | 74.75 | -97.47 | 6.1 | 16.43 | 0.21 | 10.6 | 181.7 | 0.054 | 0.021 | 0.401 | 0.015 | 0.058 |
| **CAA7** | 73.66 | -96.53 | 2.1 | 13.3 | 0.13 | 15.6 | 81.3 | 0.109 | 0.066 | 0.335 | 0.057 | 0.146 |
| **VS** | 69.16 | -100.69 | 8.4 | 8.23 | 0.18 | 10.6 | *nd* | 0.029 | 0.020 | 0.309 | 0.032 | 0.037 |

**Table 2.** Mixed layer depth (MLD), ice cover, HPLC pigment measurements (ratios of selected marker pigments to chl *a*), DMS (MIMS) and DMSP (OSSCAR) measurements. Perid = peridinin, 19'ButFuc = 19'-butanoyloxyfucoxanthin, Fuc = Fucoxanthin, 19'HexFuc = 19'-hexanoyloxyfucoxanthin, Diadino = Diadinoxanthin. *nd*= no data. *bdl* = below detection limit.

| Station | Diatom | Dinoflag. | Chloro. | Prasino | Crypto. | C-P | c3-Flag. | Hapto-7 |
|---|---|---|---|---|---|---|---|---|
| K1 | 37 | 14 | 0 | 17 | 4 | 9 | 1 | 16 |
| LS2 | 39 | 19 | 0 | 23 | 1 | 3 | 7 | 8 |
| BB3 | 48 | 15 | 4 | 14 | 8 | 1 | 5 | 5 |
| BB2 | 44 | 16 | 11 | 14 | 4 | 2 | 1 | 8 |
| CAA1 | 47 | 4 | 0 | 39 | 2 | 2 | 4 | 2 |
| CAA5 | 50 | 19 | 1 | 10 | 3 | 2 | 14 | 1 |
| CAA6 | 52 | 16 | 1 | 8 | 3 | 2 | 17 | 1 |
| CAA7 | 46 | 11 | 4 | 17 | 8 | 8 | 0 | 5 |
| VS | 67 | 8 | 0 | 11 | 3 | 3 | 6 | 3 |

**Table 3.** CHEMTAX-derived phytoplankton assemblage estimates (numbers given are percent of total chl *a*) for sampled stations. Diat. = diatoms; Dinoflag = Dinoflagellates; Chloro. = Chlorophytes; Prasino = Prasinophyte (types 2 and 3); Crypto. = Cryptophytes Chryso-Pelago =Chrysophytes/Pelagophytes; c3-flag. = c3-Flagellates; Hapto-7 = Haptophyte type 7. Due to the presence of unidentified phytoplankton taxa, not all assemblage estimates sum to 100%.

| Variable | DMS Correlation Coefficient | DMSP Correlation Coefficient |
|---|---|---|
| **$\Delta O_2$/Ar** | 0.22 | 0.33 |
| **Salinity** | 0.35 | 0.34 |
| **SST** | 0.29 | 0.14 |
| **Fluorescence** | 0.32 | 0.66 |
| ***p*$CO_2$** | 0.16 | 0.12 |
| **Ice Cover** | -0.26 | -0.34 |

**Table 4.** Pearson correlation coefficients relating DMS measurements made by MIMS and DMSP measurements made by OSSCAR to other oceanographic variables. Only correlations significant at the $p < 0.05$ level are shown. $\Delta O_2$/Ar ratios were obtained using MIMS.

| Author | Year | Month | Region | DMS (nM) | DMSP (nM) | Assemblage characteristics |
|---|---|---|---|---|---|---|
| **Bouillon et al. 2002** | 1998 | April-June | North Water | 0.04-6.7 | 0.9-53 | Diatom dominated assemblage |
| **Matrai et al. 1997** | 1993 | May | Barents Sea | 2.8 - 25.3 | 6-27 | Diatom-dominated and *Phaeocystis*-dominated stations |
| **Lizotte et al. 2012** | 2003 | May-October | Northwest Atlantic | 0.1-12 | 4-101 | Nanoflagellate dominated in all seasons |
| **Gali et al. 2010** | 2007 | July | Greenland Sea | 0.1 - 18.3 | 1.4 - 163.6 | Haptophyte (*Phaeocystis)* dominance |
| **Leck et al. 1996** | 1991 | August-October | Greenland Sea | 0.04 - 12 | -- | Not described |
| **Motard-Côté et al. 2012** | 2008 | September | Baffin Bay North Water | 0.4-5.2 | 5–70 | |
| **Scarratt et al. 2007** | 1999 | September | Northwest Atlantic | 0.2-4.7 | 0-203 | Mixed assemblage |
| **Luce et al. 2011** | 2007 | October-November | High Arctic | 0.05-0.8 | 2- 39 | Flagellate-dominated except for diatom-dominated in Baffin Bay |

**Table 5.** Compilation of published Arctic and Subarctic Atlantic DMS/P data from the summer and fall months, focusing on observations from the Western Hemisphere.

**Figures:**

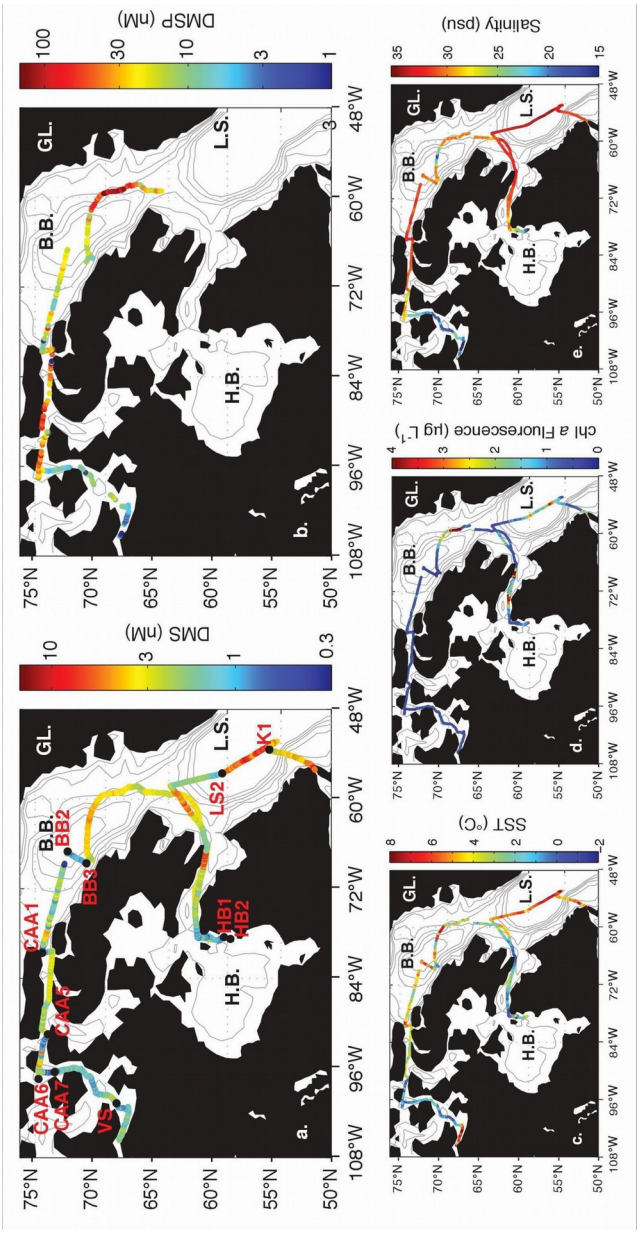


**Figure 1.** Spatial distribution of DMS, DMSP and hydrographic variables. GL. = Greenland, B.B. = Baffin Bay, L.S = Labrador Sea, H.B. = Hudson Bay, C.A.A. = Canadian Arctic Archipelago.

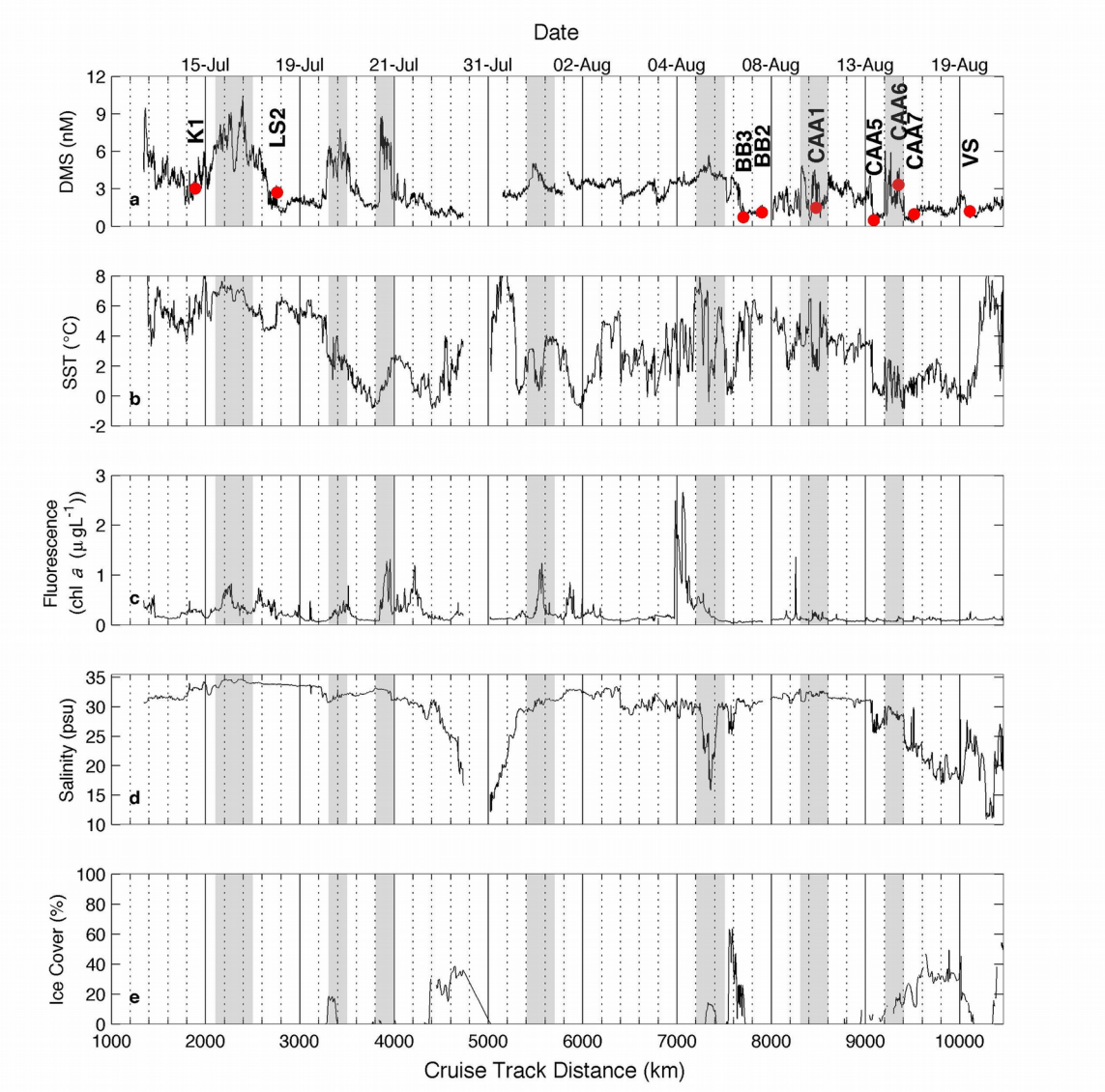


992

993 **Figure 2.** Distribution of DMS and hydrographic variables along our cruise track. Grey

994 shaded areas denote regions of sharp increases in DMS. Labeled red dots indicate

995 sampling stations (see Table 2).

996

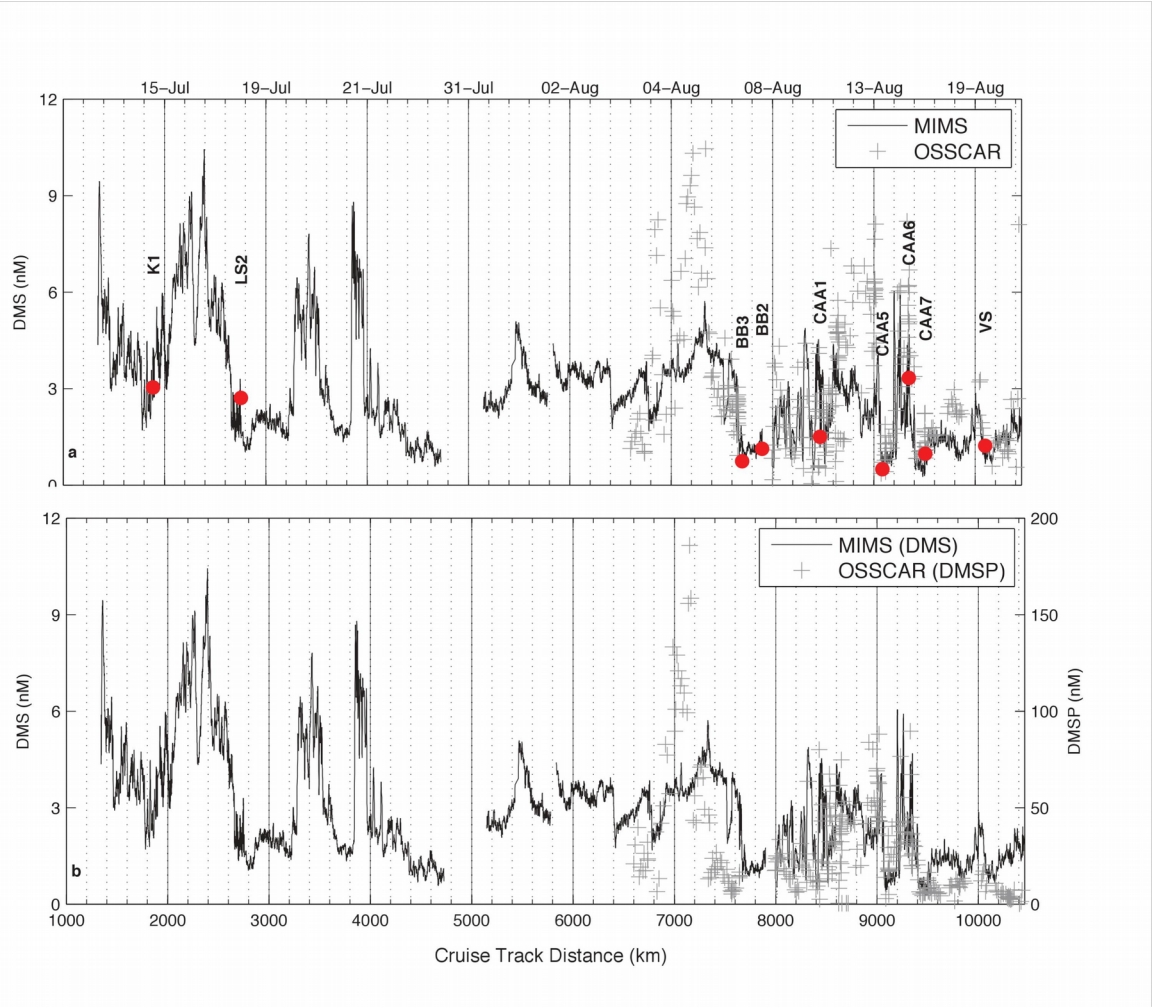


998 **Figure 3.** Distribution of DMS and DMSP along the cruise track. Panel (a) shows DMS
999 measurements made by MIMS and OSSCAR. Note that a small fraction (less than
1000 0.5%) of measurements made by OSSCAR were above 12 nM. Panel (b) shows MIMS
1001 data with OSSCAR DMSP measurements superimposed on a different y scale (right hand
1002 side). Labeled red dots indicate DMS concentrations measured at discrete sampling
1003 stations (see Table 2).
1004
1005

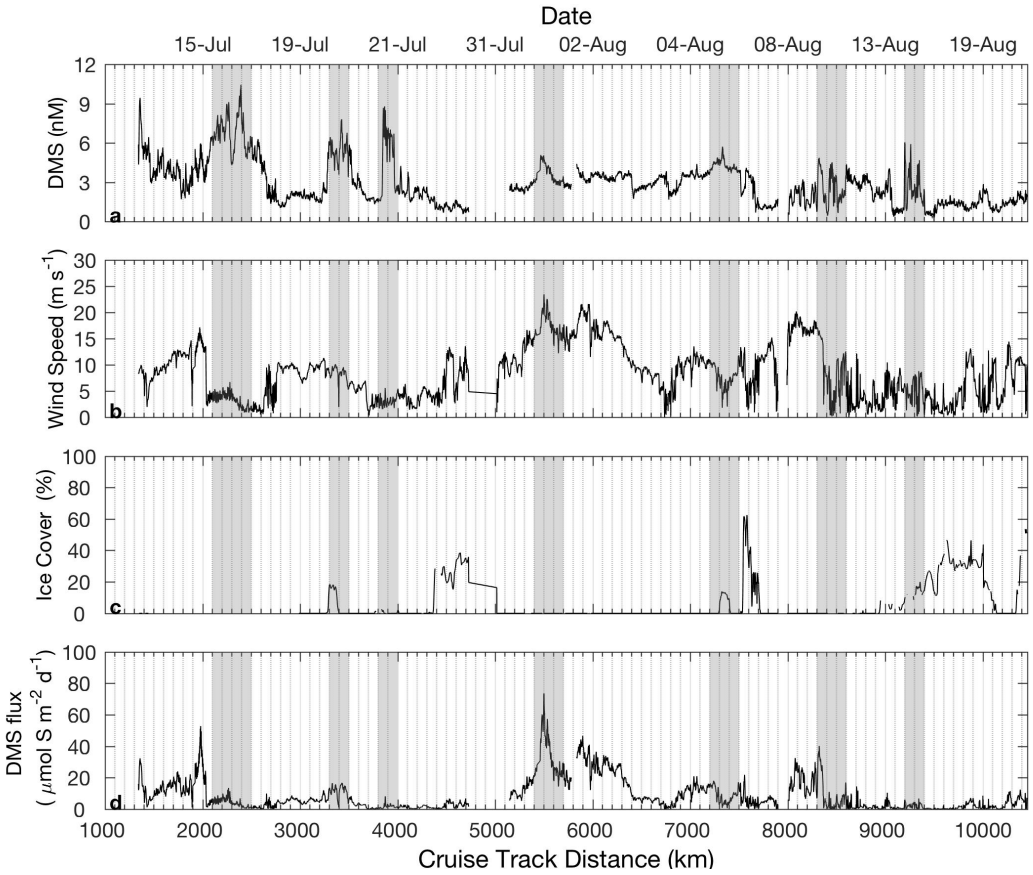


Figure 4. Distribution of DMS, wind speed, sea ice cover and sea-air DMS flux along the cruise track.

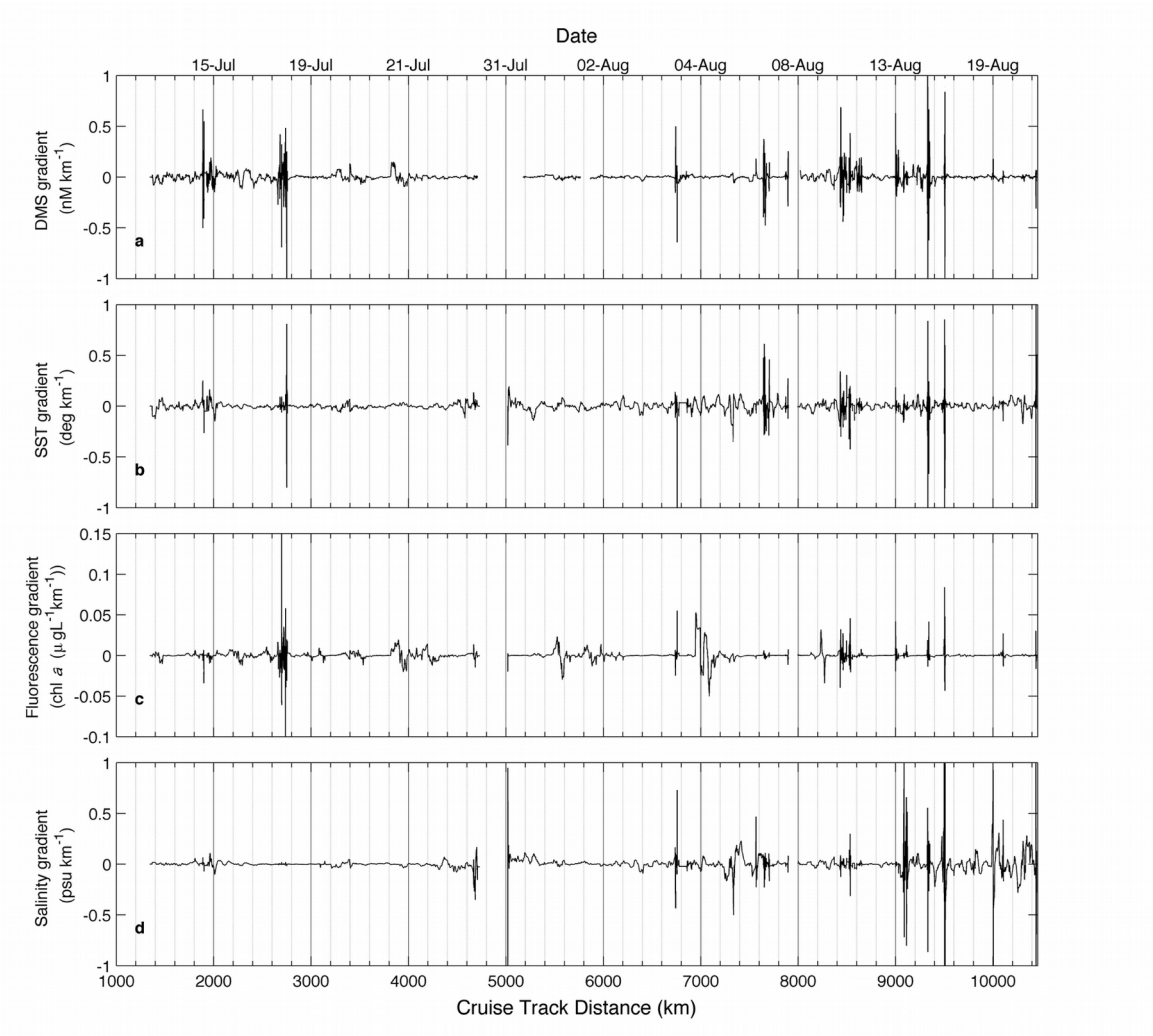


**Figure 5.** Spatial gradients in DMS (measured with MIMS) and hydrographic variables, calculated from a neighbourhood of 100 data points (~25 km).

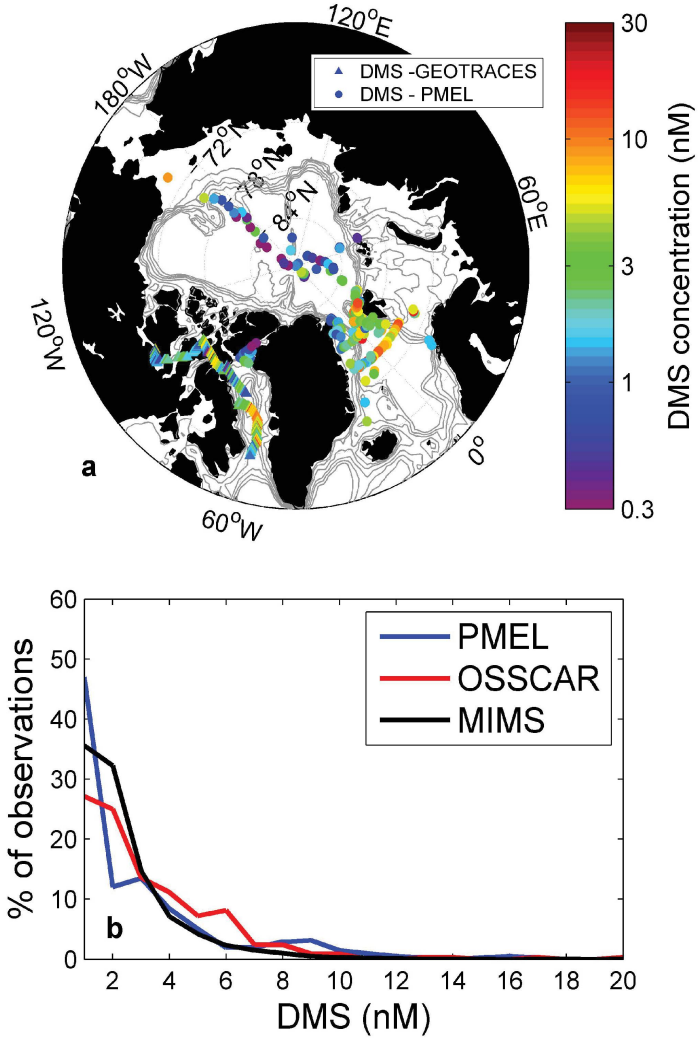


**Figure 6.** Comparison of OSSCAR- and MIMS-measured DMS from this study with existing summertime data in the PMEL database. Panel (a) shows the geographic distribution of DMS measurements in the PMEL database and those obtained by this study (using OSSCAR), while panel b) shows a histogram of DMS concentrations in three datasets – the MIMS dataset (33,250 data points) the OSSCAR dataset (344 points) , and the PMEL dataset. (415 points).